








Determining External and System Effects on Reducing Waste Output of Photovoltaic Batteries Using PV syst Software

Uygun Kholov^{1*}, Muhamad Tursunov²,
Xabibullo Sabirov¹, Mansur Eshmatov³,
Ramazan Alikulov¹, Abror Eshmatov⁴

¹Karshi State Technical University, Karshi, 18100, Uzbekistan

²S.A. Azimov Physical-Technical Institute of Uzbekistan Academy of Sciences,
Tashkent, 100084, Uzbekistan

³Turan University, Karshi, 180111, Uzbekistan

⁴Chirchik State Pedagogical University, Tashkent, 111718, Uzbekistan
uygunshams@mail.ru

Abstract. The productivity of an autonomous photovoltaic plant with a capacity of 2.7 kW, installed in the parking area, was analyzed, using the PV syst program. The modeling outcomes showed, that the highest value of the global horizontal solar radiation flux density falls on the summer season and is $\sim 214,0 \text{ kW}\cdot\text{h}/\text{m}^2$. Due to unused electrical energy, daily and monthly losses amount to 69,3%. Percentage-wise, energy losses were distributed as follows: 6,14% due to high temperature, 2,5% due to degradation of photovoltaic batteries, 2,1% in the switching points of photovoltaic batteries, and ohmic losses in wires – 1,73%. The modeling outcomes indicate the loss of electrical power, the reduction of which will lead to an efficiency improving of the autonomy photovoltaic plant.

Keywords: autonomous photovoltaic station, photovoltaic battery, solar radiation, consumer, storage battery.

1 Introduction

The Sun is a global and environmentally clean source of energy. In just one hour, the Earth receives from the Sun an amount of energy sufficient to meet the annual energy demand of humankind. The direct conversion of solar radiation into electrical energy is carried out by photovoltaic batteries (PVB) or photovoltaic power stations (PVPS). The output power of a PVB depends on the number of solar cells it contains, while the power of a PVPS depends on the number of PVBs it comprises. In other words, the capacities of PVBs and PVPSs can be increased by proportionally expanding the number of solar cells and photovoltaic modules. Electric power can be transmitted to consumers through three main methods: direct grid connection, autonomous operation, and hybrid operation. In the case of direct connection to the grid, electricity generated by the PVPS is transmitted through inverters. When the system includes storage batteries (SB), the PVPS operates autonomously, i.e., independently from the grid. If the system configuration includes both inverters and storage batteries, the PVPS can function both autonomously and in grid-connected mode, allowing for flexible operation [1]. The efficiency of converting solar radiation into electrical energy depends on the location and orientation of the PVPS as well as on the technical characteristics of its components. Formally, the design of a PVPS represents a multi-factor optimization problem aimed at achieving maximum efficiency. As is well known, such problems are typically solved using computer modeling techniques. In this study, the design of a PVPS intended for parking lot lighting was carried out using the **PVsyst** software [2, 3]. The results of the simulation were compared with the actual operational data of a real PVPS that provides lighting for a car parking area.

2. Object and research method

A solar-powered lighting system for a car parking area was designed and constructed (Fig. 1). During nighttime, the parking lot is illuminated by eight LED lamps with a total power of 144W and three additional lamps with a total power of 150W. The power supply source consists of four gel rechargeable batteries (model VG 12-200) with a capacity of 200 Ah each, connected in series. On the roof of the parking area, a PVPS is installed, consisting of 16 photovoltaic batteries, each rated at 170 W, divided into four groups.



Fig. 1. General view of the car parking area with nighttime lighting powered by a 2.7 kW PVPS

Each group includes four batteries connected in series. During the daytime, the PVPS charges the rechargeable batteries through an MPPT controller (model PC16-

6015A, 60A, 48V). At night, a 3kW inverter (Invertor 3000W SUKAM'S, 48V) converts the direct current (DC) power from the batteries into alternating current (AC) power to supply the lamps. All auxiliary equipment is mounted in a control cabinet, which is protected from external environmental influences [4]. The PVPS is oriented toward the south, and the total tilt angle (roof inclination relative to the ground plus the tilt of the PVPS relative to the roof) is 38° . During nighttime (in the evening and early morning), when the illumination level reaches 30lx or 120lx, the photo relay automatically switches the lamps on or off. The maximum power consumption of the lamps per hour is 294W, while the daily electricity consumption amounts to 2.94 kWh/day.

3. Computer modeling of the PVPS

For the design of the PVPS, the freely distributed software PVsyst [5] was selected. The PVsyst package includes a database of PVsystem components as well as the Meonorm [6] climate database, which provides climatic parameters for the specific location of the PVPS. In addition, Google Maps is used to visualize the photographic and geographical position of the designed system (Fig. 2).



Fig. 2a. Location of the PVPS: (a) satellite view, Tashkent — latitude $41^\circ20'23''$ N, longitude $69^\circ17'36''$ E, altitude 426 m above sea level, annual solar radiation flux density - 1660.1 kWh/m²/year.



Fig. 2b. Location of the PVPS: (b) map view. Tashkent — latitude $41^\circ20'23''$ N, longitude $69^\circ17'36''$ E, altitude 426 m above sea level, annual solar radiation flux density - 1660.1 kWh/m²/year.

The initial data for the design process include the amount of electricity consumption and the geographical location of the PVPS. After specifying the coordinates of the PVPS and the required energy demand, the user selects the system components from the database. The software then calculates the geometrical parameters of the system and determines the tilt angle of the PVPS (Fig. 3).

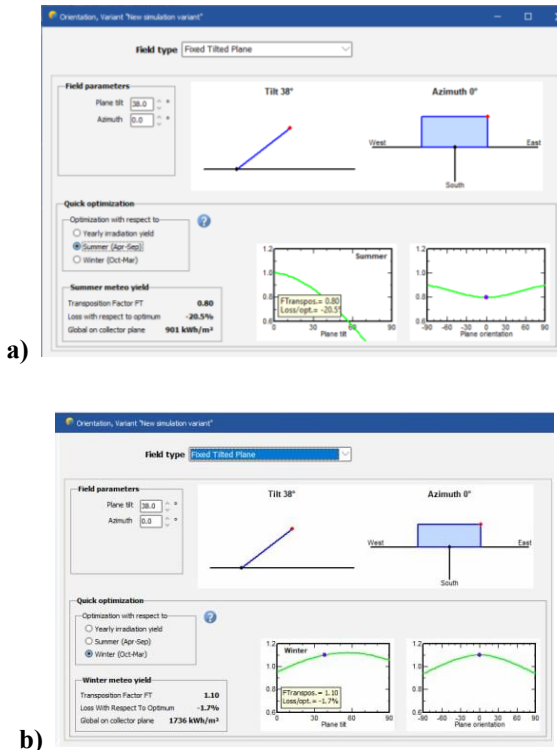


Fig. 3. Tilt and orientation of the PVBs

Table 1 presents the optimal tilt angle of the PVBs for each month.

Table 1. Average installation angle of PVBs for each month

Months	January 17	February 15	March 16	April 15	May 15	June 11	July 18	August 16	September 16	October 16	November 15	December 11
Angle	62°	54°	43°	32°	22°	18°	20°	28°	39°	51°	60°	64°

When calculating these installation angles, the geographical latitude of the location where the PVBs were installed (for Tashkent – 41°) was taken into account. The following formulas were used to determine these daily values:

$$\beta_0 = \varphi - \delta_0 \tag{1}$$

Where φ is the geographical latitude of the location (°); δ_0 is the solar declination angle for the selected month (°). To keep the front surface of the PVB always facing the Sun, the solar declination angle δ_0 is determined using Cooper’s formula [7].

$$\delta_0 = 23,45 \cdot \sin\left(360 \frac{284+n}{365}\right) \tag{2}$$

According to the calculations presented in table 2, the PVB require a dual-axis tracking system. However, installing a dual-axis tracking system will increase the cost. In this case, the price of the generated electricity will rise even more. Therefore, it is advisable to install the PVBs at an optimal angle for each season or for the whole year.

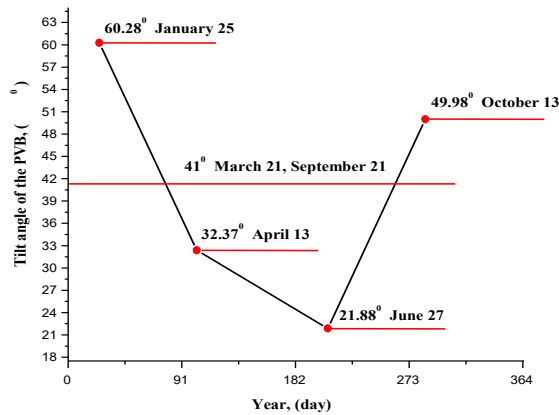


Fig. 4. Optimal installation angle of PVBs relative to the Sun by seasons of the year

In figure 4, the PVBs for each season and the annual optimal installation angles are shown. According to figure 4, the optimal installation angles of the PVBs were determined for each season (60,3° in winter on January 25, 32,4° in spring on April 13, 22,0° in summer on July 27, and 50,0° in autumn on October 13), and the annual optimal installation angle was found to be 41°. The optimal installation angle, set once a year, equals 41° for the heliopoly system of the Physical-Technical Institute in Tashkent. It was determined that the annual optimal installation angle corresponds to the geographical latitude and to the angles of the spring and autumn equinoxes at the study location.

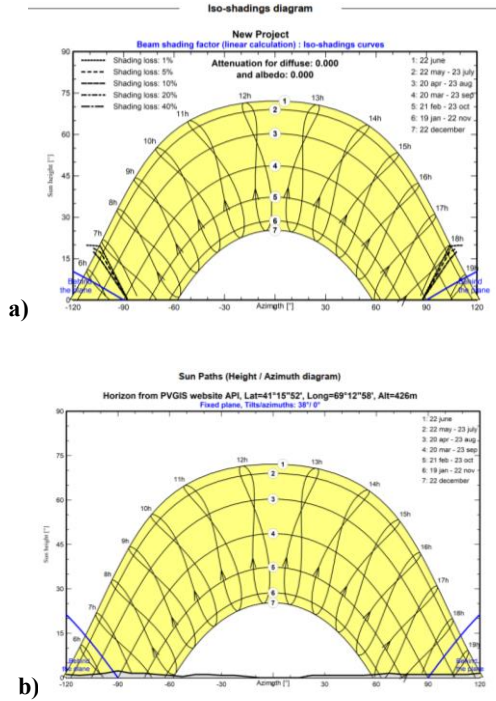


Fig. 5. Diagram of diffuse radiation and ground albedo (a), and the schematic position of the Sun relative to the horizon and azimuth (b).

The performance of a PVPS depends on the solar radiation flux density, which is determined not only by the position of the Sun in the sky (Fig. 5) but also by the seasonal variation of solar radiation (Fig. 6). It also reflects the influence of ambient temperature variation throughout the year on the performance of the PVPS; however, this factor is not analyzed in detail and is only mentioned in general terms.

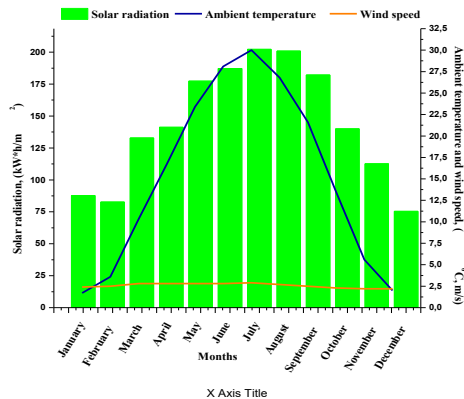


Fig. 6. Variations in solar radiation flux density, air temperature, and wind speed during the month.

Rechargeable batteries are essential components of stand-alone PVPS. The criteria for selecting SB are well known [8]. The PVsyst software automatically selects the type and number of SB. In our case, four (4) sealed lead-acid gel SB with a capacity of 200 A·h each were chosen, offering long storage life and a high number of charge/discharge cycles (Table 2). At present, the SB charging process is mainly controlled by MPPT-type controllers [9]. The inverter, which converts DC into AC, is an integral part of any PVPS regardless of the method of energy delivery to the consumer. An incorrectly selected inverter may lead to reduced system performance [10, 11]. All stages of the PVsyst modeling process are displayed on the computer screen in the form of figures, graphs, and diagrams. Table 2 presents the parameters of the selected PVBs and devices taken from the PVsyst database for the autonomous photovoltaic power station (APVPS).

Table 2. Technical parameters of the selected components from the PVsyst database for the APVPS.

Photovoltaic module		Battery	
Manufacturer	Solarfun	Manufacturer	Narada
Model	SF 190-27-M170	Model	AcmeG 12V 200
(Initial PVsyst database)		Technology	Lead-acid, sealed, Gel
Power	170 W _p	Number of units	4 in series
Number of PV panels	16	Discharge, minimum SOC	12.1 %
Nominal value (under STC conditions)	2720 W _p	Stored energy	8.7 kW·h
Modules (parallel, series)	4x 4	Battery specifications	
In operating condition, (50 °C)		Voltage	48 V
P _{mpp}	2480 W _p	Capacity	200 A·h (C10)
U _{mpp}	90 V	Temperature	Fixed 25 °C
I _{mpp}	27 A		
Controller		Battery management control	
Universal controller	Schneider Electric	Charge	54.9 / 50.2 V
Model	MPPT 60 150-48	SOC correction	0.90 / 0.59
Technology	MPPT Converter	Discharge	45.5 / 48.9V
Temperature coefficient	-2.3 mV/°C/Elem.	SOC correction	0.10 / 0.35

4. Results and Discussion

As is known, to ensure maximum electricity generation, the PVBs should be installed at the optimal tilt angle. In our case, at a tilt angle of 38°, losses from April to September reach 20% (Fig. 3a). In winter, from October to March, the losses are lower,

amounting to only 1.7% (Fig. 3b). Over the course of the year, the average loss is approximately 5%. Therefore, the PVPS should be installed at a tilt angle of 41° . An important operational characteristic of the APVPS is the **performance ratio**. The nominal power and the performance ratio of the PVBs are recorded in the datasheet. The obtained results are calculated using the following formula [12]:

$$PR_{APVPS} = \frac{E_{DEG} (kW \cdot h)}{E_{STC} (kW \cdot h)} \cdot 100\% \quad (3)$$

As is known, to ensure maximum electricity generation, the PVBs should be installed at the optimal tilt angle. In our case, at a tilt angle of 38° , losses from April to September reach 20% (Fig. 3a). In winter, from October to March, the losses are lower, amounting to only 1.7% (Fig. 3b). Over the course of the year, the average loss is approximately 5%. Therefore, the PVPS should be installed at a tilt angle of 41° . An important operational characteristic of the APVPS is the **performance ratio**. The nominal power and the performance ratio of the PVBs are recorded in the datasheet. The obtained results are calculated using the formula (3).

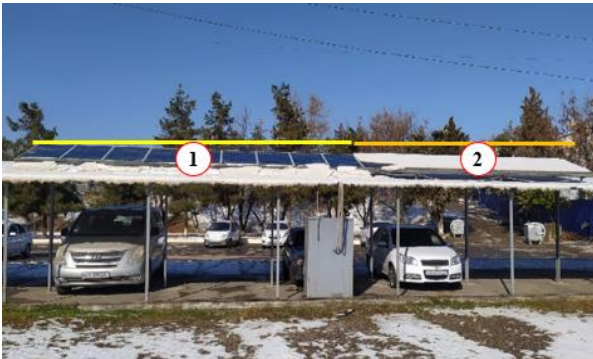


Fig. 7. 1 – Front surface of the PVB covered with polished protective glass, 2 – Front surface of the PVB covered with textured protective glass

If the front protective surface of a PVB is covered with smooth glass, the reflection coefficient of the solar radiation flux density will be higher. If the front protective surface is covered with textured glass, the reflection coefficient of the solar radiation flux density is lower (due to refraction from the textured surfaces). PVBs covered with curved glass are highly prone to soiling. Some of the dust falling on the front surface of PVBs protected by smooth glass can be removed by light wind. However, dust on the front surface of PVBs protected by textured glass cannot be removed by weak wind. This is confirmed in figure 7, where long-term snow accumulation on the front surface of PVBs in winter is observed, despite exposure to open air. Figure 8 shows the annual performance ratio and the share of solar energy of the autonomous APVPS. It can be seen that the performance ratio is minimal in the summer months, despite the fact that

the solar radiation flux density is maximal during these months (Fig. 6). The main energy losses during this period are caused by high air temperature and, consequently, the high temperature of the PVBs in the system.

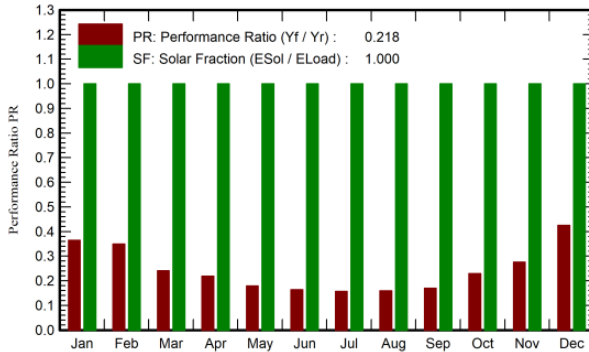


Fig. 8. Performance ratio and share of solar energy

The diagram in figure 9 illustrates the distribution of annual losses in the PVPS: losses during the transmission of electricity generated by PVBs, total losses in the SBs, the amount of electricity delivered to the consumer, and unused electricity.

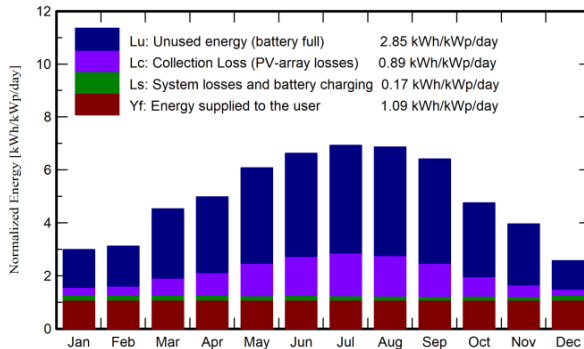


Fig. 9. Monthly electricity generation, including energy losses

The nominal power of the PVPS is 4746kWh, with an efficiency of 12%. The main sources of energy losses were identified as follows: due to PVB overheating – 6,14%, PVB degradation – 2,5%, PVB connections with elements – 2,1%, and wire resistance – 1,73%. Taking these losses into account, the volume of useful electricity produced is 1252kWh. At the inverter output, the annual amount of energy delivered to the consumer is 1082kWh [16]. It is interesting to compare the simulation results of the average monthly energy distribution with experimental data (Fig. 10). The difference between the simulation results and the experimental data for each month can be seen in figure

10. According to the simulation results, the monthly energy distribution has average values ranging from $90 \pm 2,6$ to $72,8 \pm 12,8$.

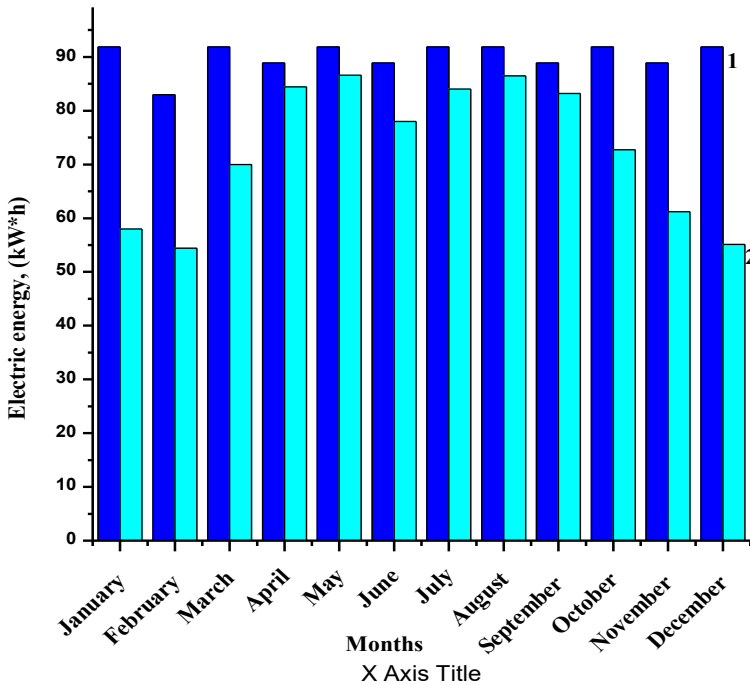


Fig. 10. Monthly electricity distribution: 1 – PVsyst simulation; 2 – experiment

5. Conclusion

Computer modeling is essential at the design stage of a PVPS. The simulation results indicate electricity losses. In this study, the performance of a 2.7kW APVPS installed at the parking lot of the Physical-Technical Institute was analyzed using the PVsyst software. The simulation results showed that the maximum value of global horizontal solar radiation flux occurs in the summer season, ranging from 201.6 to 227kWh/m², and daily and monthly losses due to unused electricity amount to 69.3%. It was found that these losses can be mitigated by connecting additional consumers. It was also established that adjusting the tilt angle of the PVBs to the solar radiation incidence angle reduces energy losses and increases performance. Analysis of the APVPS using PVsyst allows identification of all associated losses, and accounting for and minimizing them leads to increased system efficiency. Thus, studying the influence of regional climatic conditions in the Republic for each specific application of crystalline silicon-based PVB installations shows that environmental temperature, atmospheric soiling, and the topology of the protective glass surface must be considered during APVPS operation.

For citations of references, we prefer the use of square brackets and consecutive numbers. Citations using labels or the author/year convention are also acceptable. The following bibliography provides a sample reference list with entries for journal articles [1], an LNCS chapter [2], a book [3], proceedings without editors [4], as well as a URL [5].

Acknowledgments. The work was financially supported by the Ministry of Innovative Development of the Republic of Uzbekistan within the framework of the project FOT- 2026-497 “Development of the scientific basis for the creation of solar cogeneration plants based on photoelectric thermal batteries”.

Disclosure of Interests. The authors have no competing interests to declare that are relevant to the content of this article.

References

1. Jaydeep V.R. Performance Evaluation of Grid-Connected Solar Photovoltaic Plant Using PVSYSY Software. *Journal of emerging Technologies and Innovative Research (JETIR)*, Vol. 2, p. 372–378, 2015.
2. Kirpichnikova I.M., Makhsumov I.B. “Selection of Electrical Equipment for an Autonomous Photovoltaic System Using PVsyst Software”, *Bulletin of SUSU. “Energy” Series*, Vol. 20, No. 2, pp. 77–88, 2020.
3. Kianda Dhipatya Syahindra, Samsul Ma’arif, Aditya Anindito Widayat, Ahmad Fakhrul Fauzi, and Eko Adhi Setiawan. “Solar PV System Performance Ratio Evaluation for Electric Vehicles Charging Stations in Transit Oriented Development (TOD) Areas”, *E3S Web of Conferences* 231, 02002, p. 2-5, 2021, DOI: [org/10.1051/e3sconf/202123102002](https://doi.org/10.1051/e3sconf/202123102002).
4. Tursunov M.N., Sabirov Kh., Kholov U.R., Akhtamov T.Z. “Autonomous photovoltaic system for year-round guaranteed electricity supply to rural facilities”, *Journal “Irrigation and Reclamation”*, No. 3(20), pp. 82-86, 2020.
5. www.pvsyst.com date of request: Tuesday, January 31, 2023.
6. Kamal Skeiker. “Optimum tilt angle and orientation for solar collectors in Syria”, *Energy Conversion and Management* 50, p. 2439–2448, 2009.
7. Khalaf Hassan Ali. “Empirical Model for Estimating Global Solar and Diffuse Solar Radiations on Horizontal Surfaces”, *Journal of Energy Technologies and Policy*, Vol.6, No.5, p. 40-50, 2016.
8. Armstrong S., Glavin M.E., Hurley W.G. Comparison battery charging algorithms for stand-alone photovoltaic system. *Conference Paper in PESC Record - IEEE Annual Power Electronics Specialists Conference*, p. 1469–1475. 2008.
9. Idris N., Omar A.M. and Shaari S. “Stand-alone photovoltaic power system application in Malaysia”, *The 4th International Power Engineering and Optimization Conference (PEOCO2010)*, Shah Alam, Selangor, Malaysia, p. 23-24, 2010.
10. Mohammadi F., “Design and Electrification of an Electric Vehicle Using Lithium-ion Batteries,” *3rd International Conference on Electrical Engineering*, pp. 2-11, 2018.
11. A. Najah Al-Shamani, M.Y. Hj Othman, S. Mat, M.H. Ruslan, A. M. Abed, and K. Sopian, “Design and Sizing of Stand-alone Solar Power Systems A house Iraq,” *Recent Advances in Renewable Energy Sources*, April, p. 145-150, 2015.
12. Nils H. Reich, Bjoern Mueller, Alfons Armbruster, Wilfried G. J. H. M. van Sark, Klaus Kiefer and Christian Reise. “Performance ratio revisited: is PR > 90% realistic?”, *PROGRESS IN Photovoltaics: research and applications*, p. 717–726, 2012, DOI: [10.1002/pip.1219](https://doi.org/10.1002/pip.1219).

13. Tursunov M. N., Sabirov X., Xolov U. R., and Eshmatov M. “Investigation of the Parameters of a Photovoltaic Thermal Battery in Extreme Natural Conditions”, *Applied Solar Energy*, Vol. 57, No. 4, p. 272–277, 2021.
14. M. N. Tursunov, V. G. Dyskin, Kh. A. Sobirov, and B. M. Turdiev. “Improvement of the Efficiency of PhotoHeat Converting Plant Operation”, *Applied Solar Energy*, 2014, Vol. 50, No. 4, p. 287–288.
15. Figgis, B.; Scabbia, G.; Aissa, B. Condensation as a predictor of PV soiling. *Sol. Energy*, 238, 30–38, 2022.
16. Tursunov M. N., Dyskin V. G., Yuldashev I. A., Sobirov Kh., and Park Jeong Hwoan. “A Criterion of Contamination of the Glass Surface of Photovoltaic Batteries”, *Applied Solar Energy*, Vol. 51, No. 2, pp. 163–164, 2015.

Open Access This chapter is licensed under the terms of the Creative Commons Attribution-NonCommercial 4.0 International License (<http://creativecommons.org/licenses/by-nc/4.0/>), which permits any noncommercial use, sharing, adaptation, distribution and reproduction in any medium or format, as long as you give appropriate credit to the original author(s) and the source, provide a link to the Creative Commons license and indicate if changes were made.

The images or other third party material in this chapter are included in the chapter's Creative Commons license, unless indicated otherwise in a credit line to the material. If material is not included in the chapter's Creative Commons license and your intended use is not permitted by statutory regulation or exceeds the permitted use, you will need to obtain permission directly from the copyright holder.

